Food Chemistry: X 24 (2024) 101854

Contents lists available at ScienceDirect

Food Chemistry: X

journal homepage: www.sciencedirect.com/journal/food-chemistry-x

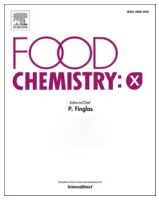

Potassium chloride-assisted heat treatment enhances the de-glycosylation efficiency and xanthine oxidase inhibitory activity of *Sophora japonica* L. flavonoids

Jun Li [a,b,c], Peng Wu [b,c], Jing Wang [b,c], Xiangren Meng [b,c,*], Yang Ni [a], Liuping Fan [a,**]

[a] School of Food Science and Technology, Jiangnan University, 1800 Lihu Avenue, Wuxi, Jiangsu 214122, China
[b] Chinese Cuisine Promotion and Research Base, Yangzhou University, Yangzhou 225127, China
[c] College of Tourism and Culinary Science, Yangzhou University, Yangzhou 225127, China

ARTICLE INFO

Keywords:
Flavonoid composition
Salt
Degradation
Flos Sophorae Immaturus tea
Artificial neural network

ABSTRACT

Salt-assisted heat treatment is considered an effective way to enhance the bioactivities of flavonoids in *Flos Sophorae Immaturus* tea (FSIt). Herein, sodium chloride (NaCl)- and potassium chloride (KCl)-assisted heat treatment was employed to process FSIt, the components, xanthine oxidase (XO) inhibitory activity, and degradation or conversion kinetics of FSIt flavonoids were recorded. Results showed that KCl-assisted heat treatment significantly increased the XO inhibition rate of FSIt from 28.05 % to 69.50 %. The de-glycosylation of flavonoids was the crucial reason for enhancing XO inhibitory activity. Notably, KCl exhibited a better catalytic effect on the de-glycosylation reaction than NaCl. Meanwhile, conversion kinetics showed that the generation rate of quercetin, kaempferol, and isorhamnetin reached the maximum at 180, 160, 160 °C, respectively. Furthermore, the established artificial neural network model could accurately predict the changes of FSIt flavonoids during salt-assisted heat treatment. Thus, KCl can be used as a valuable food processing adjuvant to enhance the bioactivities of food materials.

1. Introduction

Flos Sophorae Immaturus tea (FSIt) is consumed as a functional beverage in China, which derives from the dried flower buds of *Sophora japonica* L. (Gong, Fan, Wang, & Li, 2023). FSIt is rich in various phenolic compounds, mainly composed of flavonoids, including rutin (RU), narcissoside (NA), kaempferol-3-*O*-rutinoside (KAr), etc. (Wang et al., 2020). Moreover, various studies confirmed that FSIt exhibited antioxidant, antiviral, analgesic, anti-hyperuricemia, and hemostasis properties (He et al., 2016; Huo et al., 2023). Multiple studies also showed that plant polyphenols exhibited a good impact on human and animal health, such as antidiabetic (Abduallah, Ahmed, Bajaber, & Alalwiat, 2023), antimicrobial (Dalal, Kunte, Oblureddy, & Anjali, 2023; Saleh, Ramadan, Elmadawy, Morsi, & El-Akabawy, 2023), immunomodulatory (Abbas & Alkheraije, 2023), improved spermatozoa quality (Bebas, Gorda, & Agustina, 2023), protective effect of DNA damage, nephrotoxicity and biochemical parameters (Turan et al., 2023), etc. However, polyphenols in plant materials exposed a series of disadvantages, such as poor water solubility, low bioavailability, and poor processing stability, which limited their effective bioactivities (Premathilaka, Rashidinejad, Golding, & Singh, 2022). Therefore, researchers are attempting to improve the bioactivities of polyphenols through heat treatments. Yu et al. (2020) found that ultrasound (600 W, 30 min) and heat treatments (150 °C, 30 min) enhanced the anti-tyrosinase ability of polyphenols from Asparagus, which might attribute to the newly formed compounds of 2-hydroxy-3-(3-hydroxy-4-methoxy-phenyl)-propionic acid 4-(2,3-dihydroxy-propyl)-phenyl ester. Xie et al. (2022) reported that steam explosion (1.6 MPa, 90 s) significantly increased the bio-accessibility, antioxidant, and antidiabetic capacity of polyphenols from hulless barley, which might be caused by the evaluated polyphenol content through processing. Meanwhile, our previous research also found that hydrothermal treatment (>160 °C, 90 min) can lead to the degradation or conversion of polyphenols in FSIt, thereby significantly improving its xanthine oxidase

* Corresponding author at: College of Tourism and Culinary Science, Yangzhou University, Yangzhou 225127, China.
** Corresponding author.
E-mail addresses: xrmeng@yzu.edu.cn (X. Meng), fanliuping@jiangnan.edu.cn (L. Fan).

https://doi.org/10.1016/j.fochx.2024.101854
Received 10 July 2024; Received in revised form 20 September 2024; Accepted 23 September 2024
Available online 24 September 2024

(XO) inhibitory activity (Li, Gong, Li, & Fan, 2023). Thus, increasing the content or improving the composition of polyphenols through heat treatment was a feasible approach to improve the bioactivities of polyphenols. However, the existing processing method also possessed disadvantages, such as a low polyphenol conversion rate and high processing loss. Although there have been studies indicating that rutin can be converted into quercetin through thermal degradation. Unfortunately, there is a lack of relevant studies on promoting efficient conversion of flavonoids through processing. Therefore, it is a meaningful topic to find a high-efficiency catalyst that can assist the conversion of polyphenols through heat treatment.

Stir-frying with salt, also called "Yanzhi" in China, is a traditional processing method for food materials and Chinese medicine. The traditional "Yanzhi" process involves soaking the materials in sodium chloride and assisting with heat treatment (Li et al., 2021). Accumulating evidence confirmed that stir-frying with salt could enhance the bioavailability and promote the conversion of phenolic acids, flavonoids, saponins, and other compounds, which was an effective way to enhance their bioactivities (Chen et al., 2018; Mubaiwa, Fogliano, Chidewe, & Linnemann, 2019). Doniec, Florkiewicz, Socha, and Filipiak-Florkiewicz (2021) indicated that boiling with the addition of sodium chloride (NaCl) and potassium chloride (KCl) significantly decreased the polyphenols content in *Brassica vegetables*, especially caffeic acid. Our previous experiments found that KCl combined with heat treatment significantly enhanced the XO inhibitory activity of FSIt compared with single heat treatment, but its mechanism was still unclear. XO is the key rate-limiting enzyme to control the generation of uric acid in the body. Studying the impact of the processing method on the XO inhibitory activity of FSIt exhibits great application value for the development of anti-hyperuricemia food derived from FSIt.

Therefore, the present study aims to maximize the functional characteristics of FSIt by improving the traditional processing technique "Yanzhi". The effect of NaCl/KCl-assisted heat treatment on the XO inhibitory activity and content of FSIt flavonoids was investigated. The mechanism of salt-assisted heat treatment improved the XO inhibitory activity of FSIt was clarified by tracking the changes in the FSIt flavonoid composition. Meanwhile, the degradation or conversion kinetic model was also created to evaluate the half-life, reaction constant, and activation energy of FSIt flavonoids. Furthermore, an artificial neural network (ANN) model was established to predict the change of FSIt flavonoid composition during salt-assisted heat treatment, thereby accurately predicting the processing conditions of FSIt with strong XO inhibitory activity. Overall, the directed conversion of flavonoids has broad application prospects in achieving precise nutrition rich in polyphenolic raw materials.

2. Materials and methods

2.1. Materials

Dried FSIt was purchased from Hebei Anguo Yao Yuan Trading Co., Ltd. (Baoding, China). RU, KAr, NA, Quercitrin (QUi), Hyperoside (HY), Quercetin (QU), Kaempferol (KA), Isorhamnetin (IS), and XO (9.1 u/mg) were acquired from Yuanye Biological Technology Co., Ltd. (Shanghai, China), and the purity of standard flavonoids was ≥98 %. Xanthine, NaCl, and KCl were obtained from Sinopharm Chemical Reagent Co., Ltd. (Shanghai, China).

2.2. Preparation of FSIt flavonoids extract

Firstly, the dried FSIt and NaCl or KCl solution was mixed in a ratio of 1:2, and the salt concentrations were 2.5 %, 5 %, and 10 % (*w*/w), respectively. The mixture was kept at room temperature for 2 h, then the surface moisture of FSIt was removed by absorbent paper. Secondly, the heat treatment was performed using a hot air oven (Binder, Neckarsulm, Germany) at 180 °C for 60 min (Li, Gong, Li, & Fan, 2023a). The sun-dried FSIt was assigned as control group 1 (CG1), and the FSIt dried at 180 °C for 60 min without salt soaked was assigned as control group 2 (CG2). Thirdly, the dried FSIt was smashed and passed through an 80 mesh-sieve, and the flavonoids of samples were extracted using 70 % (*v*/v) ethanol at a solid-liquid ratio of 1:400. The extraction was performed by a magnetic stirrer (IKA, Staufen, Germany) at 300 rpm for 40 min, then the mixture was centrifuged at 6000 rpm for 10 min, and the supernatant was collected. The residues were extracted three times. Finally, the supernatant was merged and evaporated by a rotary evaporator (IKA, Staufen, Germany) at 55 °C. The samples were re-dissolved to 100 mL with methanol and placed at 4 °C until analysis.

2.3. Determination of flavonoids

The total flavonoid content (TFC) and total polyphenol content (TPC) were determined by the aluminum chloride colorimetric method and Folin-Ciocalteu method, respectively (Chao & Fan, 2023). The flavonoid composition was analyzed by the HPLC method according to our previous study (Li, Gong, Li, & Fan, 2023b).

2.4. Determination of the XO inhibition rate

An HPLC instrument (Shimadzu, Kyoto, Japan) equipped with a C18 column (4.6 mm × 250 mm × 5 μm) and UV detector was employed to measure the XO inhibition rate according to the previous study with minor revisions (Liu et al., 2020). Briefly, the mixture comprised of 50 μL sample solution (from 0 to 1.0 mg/mL), 50 μL xanthine solution (1.0 mM), and 800 μL phosphate buffer solution (100 mM, pH 7.4) were incubated at 37 °C for 5 min, then 100 μL XO solution (0.036 u/mL, dissolved in 100 mM phosphate buffer solution) was added and incubated at 37 °C for 30 min, finally 125 μL 12 % $HClO_4$ (aq, *w*/w) was added to terminate the reaction. The uric acid content of the sample was analyzed by the HPLC method after passing through a 0.22 μm water syringe filter. The liquid chromatography conditions were as follows: solvent A (water containing 0.1 % phosphoric acid) and solvent B (methanol) eluted at an equal gradient of 85:15; wavelength, 292 nm; column temperature, 30 °C. The phosphate buffer solution was used as the negative control group. The XO inhibitory activity was calculated as follows:

$$XO\ inhibition\ rate\ (\%) = 100\% \times \frac{C_{nc} - C_s}{C_{nc}} \quad (1)$$

where the C_{nc} and C_s denote the uric acid content of negative control group and sample group, respectively.

2.5. Model experiment of flavonoids conversion

A UPLC-QTOF-MS (Waters, Milford, USA) instrument equipped with a C18 column (2.1 mm × 150 mm × 1.7 μm) was employed to identify the degradation products of RU, QUi, HY, KAr, and NA after salt-assisted heat treatment (Zhang, Li, Fan, & Duan, 2020). The liquid chromatography conditions were as follows: solvent A, water containing 0.1 % acetic acid; solvent B, acetonitrile; flow rate, 0.3 mL/min; elution was performed with 2 % B for 1 min, from 2 % to 20 % B in 7 min, from 20 % to 30 % B in 7 min, from 30 % to 80 % B in 1 min, from 80 % to 100 % B in 1 min, from 100 % to 2 % B in 3 min. The mass spectrometer conditions were as follows: mode, negative-ion; mass, 50–1500 Da; cone, 30 V; collision energy, 25 eV; de-solvation temperature, 400 °C; source temperature, 100 °C; de-solvation gas (N_2) flow rate, 700 L/h. The conversion rates (R_c) of flavonoids were calculated by the Eq. (2):

$$R_c\ (\%) = 100\% \times \frac{C_n}{C_i} \quad (2)$$

where the C_n and C_i denote the newly formed and initial flavonoids content, respectively.

2.6. Degradation and conversion kinetics of flavonoids

The kinetics of the primary flavonoids in FSIt during salt-assisted heat treatment at different times (from 30 to 150 min) and temperatures (from 140 to 220 °C) were evaluated using a first-order kinetic model (Abi-Khattar et al., 2022).

$$ln\frac{C_t}{C_0} = -kt \tag{3}$$

where C_0 denotes the initial flavonoids content, C_t denotes the flavonoids content at t time, t represents the reaction time (min), k represents the reaction constant (min^{-1}).

Moreover, the half-life ($t_{1/2}$) and activation energy (Ea) were calculated according to Eqs. (4)–(5) (Kim, Kim, & Kim, 2022):

$$t_{1/2} = -\frac{ln0.5}{k} \tag{4}$$

$$\ln k = lnK_0 - \frac{E_a}{RT} \tag{5}$$

where T represents the absolute temperature (K), K_0 represents the prefactor, R equal to 8.314×10^{-3} (kJ/mol·K).

2.7. ANN modelling

An ANN model was established and trained with the "pytorch" network library in the Python programming language (Ulger & Delik, 2023). The structure of ANN was comprised of input layer, multiple hidden layers, and output layer. In this model, the heating temperature and time of salt-assisted heat treatment were assigned as input layers, and the flavonoids content were assigned as output layers. The dataset was randomly divided into three groups including training (70 %), validation (15 %), and testing (15 %). The model was created by learning and verifying on the training and validation groups, thereby adjusting hyper-parameters and parameter weights for best prediction results, then evaluating on the testing group to provide the final performance metrics. The parameters of ANN model were as follows: activation, relu; learning rate, dynamic self-adapting with the maximum of 0.1; hidden layer, 4; maximum number of iterations, 1000; solver, optimizer adamw. The root mean square error (RMSE) and correlation coefficient (R^2) values were employed to evaluate the established ANN model performance (Chao & Fan, 2023; Patruni & Rao, 2023).

$$RMSE = \frac{\sqrt{\sum_{i=1}^{n}(Y_a - Y_p)^2}}{n} \tag{6}$$

$$R^2 = 1 - \frac{\sum_{i=1}^{n}(Y_a - Y_p)^2}{\sum_{i=1}^{n}(Y_a - Y_m)^2} \tag{7}$$

where the Y_a, Y_p, Y_m denote the actual, prediction, and mean values of the neural network, respectively; n denotes the number of input sample.

2.8. Statistical analysis

The experimental data were analyzed by Origin (version 2018) and SPSS (version 24) software, and expressed as mean ± standard deviation (SD) in at least three independent experiments. The statistical significance was calculated by One–way variance method (ANOVA) and presented as $p < 0.05$ (Li et al., 2023a).

3. Results and discussion

3.1. XO inhibitory activity of FSIt

Our previous study verified that the XO inhibition rate of flavonoids in FSIt were significantly enhanced after heating at 180 °C for 30–150 min (Li et al., 2023a). Therefore, heat treatment was a feasible approach to enhance the XO inhibitory activity of FSIt. Herein, the salt was innovatively combined with heat treatment to further enhance the XO inhibitory activity of FSIt. As shown in Fig. 1A, NaCl or KCl-assisted heat treatment significantly increased the XO inhibition rate from 28.05 % (CG1) to 65.17 % (5 % NaCl added) or 69.50 % (5 % KCl added), respectively. Compared to the CG2 group, both KCl and NaCl exhibited a significant promoting effect on the XO inhibitory activity of FSIt, especially KCl. The enhanced XO inhibitory activity of FSIt was closely related to its flavonoid content and composition. The NaCl/KCl-assisted heat treatment caused an increase in the dissolution rate of flavonoids in FSIt, which might be one of the reasons for improving the XO inhibitory activity (Bai et al., 2021). In addition, the flavonoid composition of FSIt might change after NaCl/KCl-assisted heat treatment, and the structure of flavonoids significantly affected their XO inhibitory activity (Lin, Zhang, Liao, Pan, & Gong, 2015; Singh et al., 2019).

NaCl and KCl are usually used as spices to enhance the flavor of dishes. In traditional Chinese dietary habits, salt was added in the final stage of cooking to prevent its decomposition and preserve the original flavor. Interestingly, this study found that NaCl and KCl could serve as catalysts to improve heat treatment efficiency. Similar studies showed that graphene oxide improved the thermal efficiency of microwave (MW) irradiation, resulting in a high conversion rate of RU into QU (Sasaki et al., 2023). Overall, NaCl and KCl may serve as effective catalysts for the degradation and conversion of flavonoids during heat treatment, thereby affecting the flavonoid composition of FSIt and enhancing its XO inhibitory activity. However, their complex mechanisms still need further verification.

3.2. Flavonoids contents of FSIt

The TPC and TFC were measured to elucidate the dominant mechanism of increased XO inhibitory activity. As shown in Fig. 1B and C, compared to CG1 and CG2, the TPC and TFC showed a significant downward trend after salt-assisted heat treatment, which was opposite to the change in XO inhibitory activity. The correlation analysis results also showed a significant negative correlation between TFC (−0.64), TPC (−0.79) and XO inhibition rate (Fig. 1D). This phenomenon precisely verified that the degradation and conversion of flavonoids caused by salt-assisted heat treatment was the dominant reason for improving XO inhibitory activity.

The flavonoids in FSIt mainly consisted of RU, HY, QUi, QU, KAr, KA, NA, and IS (Li et al., 2023a). Thus, these flavonoids contents variation were tracked to further investigate the mechanism of flavonoid composition that affected XO inhibitory activity (Fig. 2). Compared to CG1, heat treatment significantly reduced the content of RU, HY, QUi, KAr, NA, and significantly increased the content of QU, KA, IS. Meanwhile, according to the molecular structure of flavonoids (Fig. 2 insert), RU, QUi, and HY were equal to QU added a glycosidic bond, KAr was equal to KA added a glycosidic bond, and NA was equal to IS added a glycosidic bond. Therefore, it could be speculated that there were three pathways for the changes in these primary flavonoids: (1) RU, HY, and QUi degraded and converted to QU, (2) KAr degraded and converted to KA, (3) NA degraded and converted to IS. The de-glycosylation of flavonoids with glycosidic bonds during heat treatment has been confirmed by previous studies. Kim and Lim (2017) reported that rutin was converted to isoquercetin and quercetin at 171.4 °C for 10 min. Another study found that cyanidin-3-glucoside and cyanidin-3-rutinoside exhibited the highest degradation rate at 125 °C, but the degradation products were not identified (Sui, Yap, & Zhou, 2015). Most studies found that the occurrence of de-glycosylation required appropriate heating conditions (temperature and time). However, the loss of flavonoids during the de-glycosylation process was often ignored, and low conversion rates caused a decrease in the bioactivities of the final product.

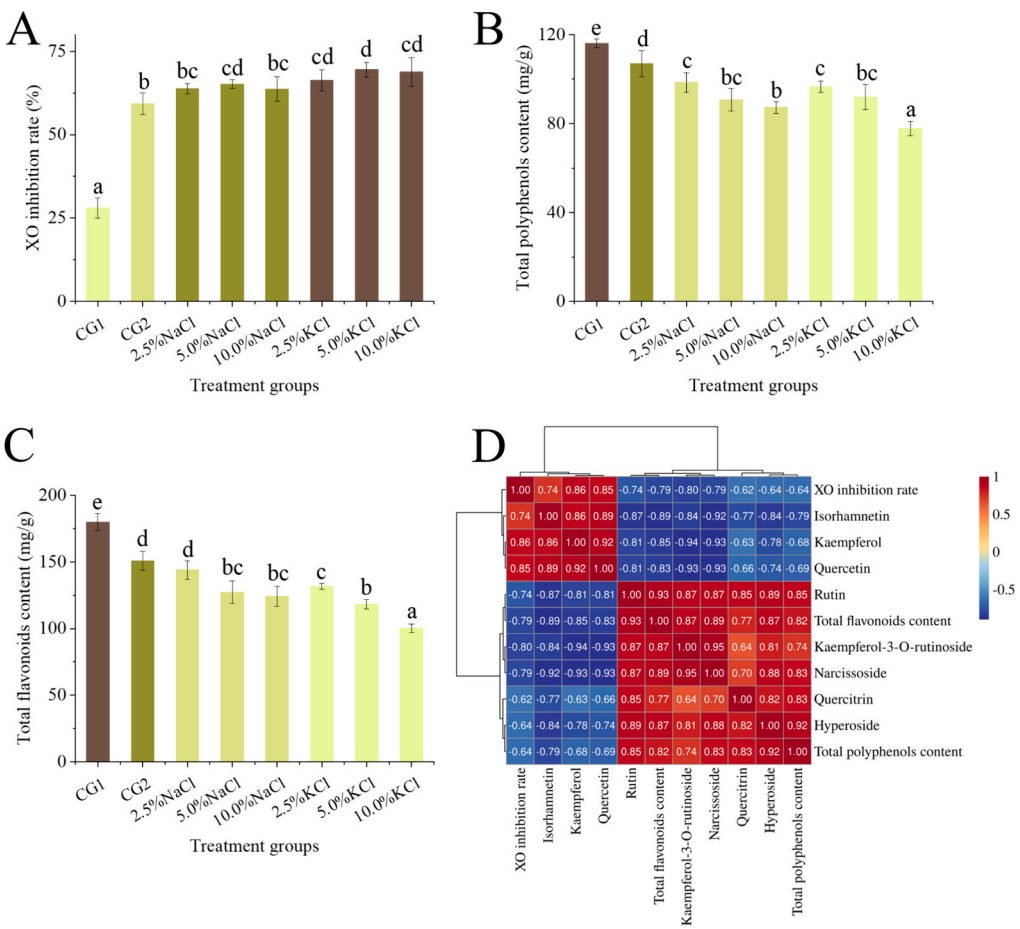

Fig. 1. Effects of salt-assisted heat treatment on XO inhibition rate (A), total polyphenols content (B), total flavonoids content (C) of *Flos Sophorae Immaturus* tea extract. Correlation analysis of XO inhibition rate, total polyphenols content, total flavonoids content, and primary flavonoids content (D). Different letters in the same graph indicate significant differences ($p < 0.05$).

Thus, suitable reaction catalysts were also one of the ways to improve the efficiency of de-glycosylation except for heating temperature and time. After heat treatment (180 °C for 15 min) combined with a kind of catalyzer (graphene oxide prepared by Tour's method), the RU conversion rate reached 98.8 % and QU yield reached 81.9 % according to the previous study (Sasaki et al., 2023). Interestingly, after combining salt and heat treatment, the degradation of RU, HY, QUi, KAr, and NA was more significant, while the increase of QU, KA, and IS was more pronounced. Compared to CG2, 5 % KCl-assisted heat treatment increased the degradation rate of RU from 42.87 % to 72.99 %, HY from 36.19 % to 47.03 %, QUi from 33.12 % to 41.60 %, KAr from 71.08 % to 83.35 %, NA from 48.30 % to 80.40 %. Conversely, the QU content increased from 22.05 to 38.32 mg/g, KA content increased from 2.02 to 2.65 mg/g, and IS content increased from 7.84 to 9.90 mg/g. Moreover, KCl exhibited stronger effect on flavonoids content than NaCl. Dhlakama, Chawafambira, and Tsotsoro (2022) showed that monovalent salts (NaCl, $NaHCO_3$) promoted the solubilization of flavonoids in Baobab (*Adansonia digitata* L.) seeds, thereby enhancing their antioxidant activity. Similar study also found that ammonium sulfate-*co*-assisted microwave method exhibited a higher extraction rate and a richer variety of polyphenols in the extraction of grape seed polyphenols (Jia, Fu, Deng, Li, & Dang, 2021). However, more studies are needed to confirm the phenomenon of salt assisted de-glycosylation of flavonoids. Importantly, the present study indicated that KCl was a good catalyst for promoting the degradation and conversion of flavonoids during heat treatment.

3.3. Degradation of primary flavonoids

To further demonstrate that de-glycosylation was the primary reason for enhancing XO inhibitory activity, the degradation processes of RU, HY, QUi, KAr, and NA during salt-assisted heat treatment were simulated. The newly formed products were identified and presented in Fig. 3A–E and Table S1. The degradation products of RU, HY, and QUi showed a $[M\text{-}H]^-$ of 301, which was identified as QU, as well as the degradation products of KAr and NA were identified as KA and IS, respectively. Meanwhile, the promotion effect of NaCl and KCl on the de-glycosylation of flavonoids was compared by calculating their conversion rates. As shown in Fig. 3A1–E1, KCl presented the highest conversion rate in the degradation process of RU (27.04 %), KAr (16.74 %), and NA (21.56 %). Moreover, KCl exhibited the same advantages in the degradation process of HY (28.69 %). However, the conversion rate of four flavonoids was not significantly improved by NaCl. This phenomenon demonstrated that KCl was a strong catalyst for promoting the degradation of 3–*O*–rutinoside and 3–*O*–galactoside, followed by NaCl. Interestingly, NaCl exhibited a better conversion rate in the degradation process of QUi than KCl, indicating that the monovalent salt ions possessed specificity for the decomposition of three glycosidic bonds (3–*O*–rutinoside, 3–*O*–galactoside, and 3–*O*–rhamnoside). NaCl solution exhibited well dielectric properties and significantly affected heat conduction efficiency during heat treatment (Xiao & Tang, 2021). However, our previous experiments found that high concentrations of NaCl (10 % added) and KCl (10 % added) did not accelerate the heating efficiency (Fig. 2), which might attribute to the threshold between ion concentration and thermal conductivity, excessively high ion concentration did

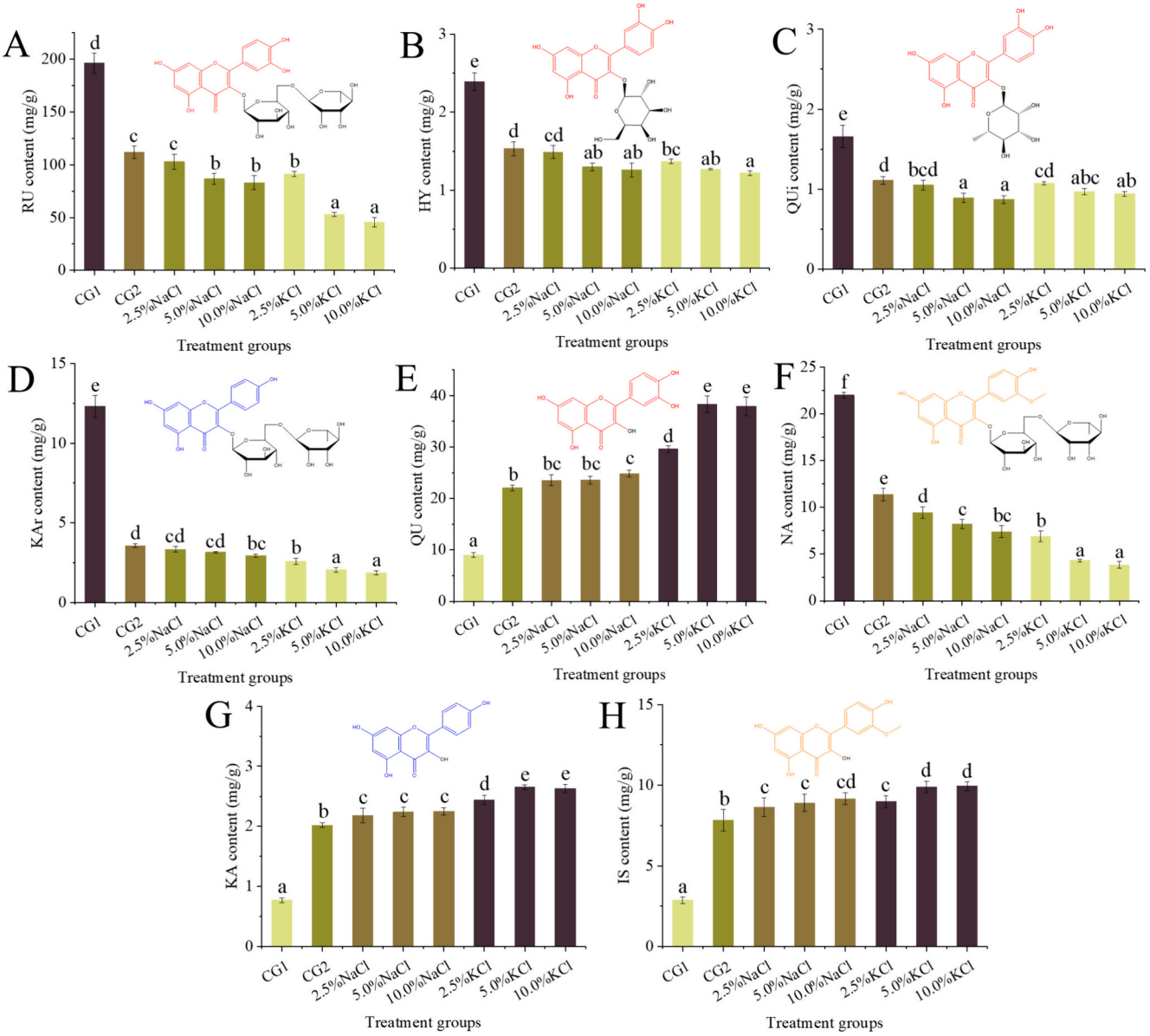

Fig. 2. Effects of salt-assisted heat treatment on the content of primary flavonoids (A, rutin; B, hyperoside; C, quercitrin; D, kaempferol–3–O–rutinoside; E, quercetin; F, narcissoside; G, kaempferol; H, isorhamnetin) in *Flos Sophorae Immaturus* tea extract. Different letters in the same graph indicate significant differences ($p < 0.05$).

not further improve its thermal conductivity efficiency (Xiao & Tang, 2021). In addition, the atomic radius of K^+ and Na^+ were different, resulting in different kinds and sizes of forces when interacting with cellulose, flavonoids and other substances, thereby affecting the efficiency of de-glycosylation of flavonoids (Yang et al., 2020).

3.4. Changes in XO inhibitory activity of simulated flavonoids

To further clarify that the de-glycosylation of five flavonoids was the primary reason for enhancing XO inhibitory activity of FSIt, the XO inhibition rates of five flavonoids before and after salt-assisted heat treatment were measured. As shown in Fig. 3A2–E2, the XO inhibitory activities of RU, HY, QUi, KAr, and NA after KCl-assisted heat treatment were significantly higher than that of CG1 and CG2 groups, indicating that the newly formed compounds of QU, KA, and IS exhibited stronger XO inhibitory activity. Meanwhile, the results of correlation analysis showed a positive correlation between QU, KA, IS and XO inhibition rate, while the content of RU, HY, QUi, KAr, NA was negatively correlated with XO inhibition rate (Fig. 1D). The XO inhibitory activity of flavonoids is significantly correlated with their structure. The C6-C3-C6 structure and the C2 = C3 double bonds of flavonoids were advantageous for XO inhibitory activity. However, the methylation, hydroxylation, and bulky sugar substitutions of flavonoids were unfavorable for XO inhibitory activity (Lin et al., 2015). Meanwhile, the quantity and position of hydroxyl groups on the benzene ring also affected the XO inhibitory activity of flavonoids (Xie et al., 2017). Overall, the de-glycosylation of flavonoids caused by salt-assisted heat treatment is a feasible approach to enhance XO inhibitory activity.

3.5. Degradation and conversion kinetics of flavonoids

The kinetic parameters and curves were carried out to explore the degradation and conversion characteristics of flavonoids in FSIt (Fig. 4 and Table 1). The degradation and conversion curves of flavonoids fitted by the first-order kinetic model showed a good linearity in the range of 140–220 °C. The k values of RU and HY reached maximum at 200 °C, and the k values of QUi reached maximum at 180 °C, while $t_{1/2}$ showed an opposite trend, indicating that RU, HY, and QUi reached the

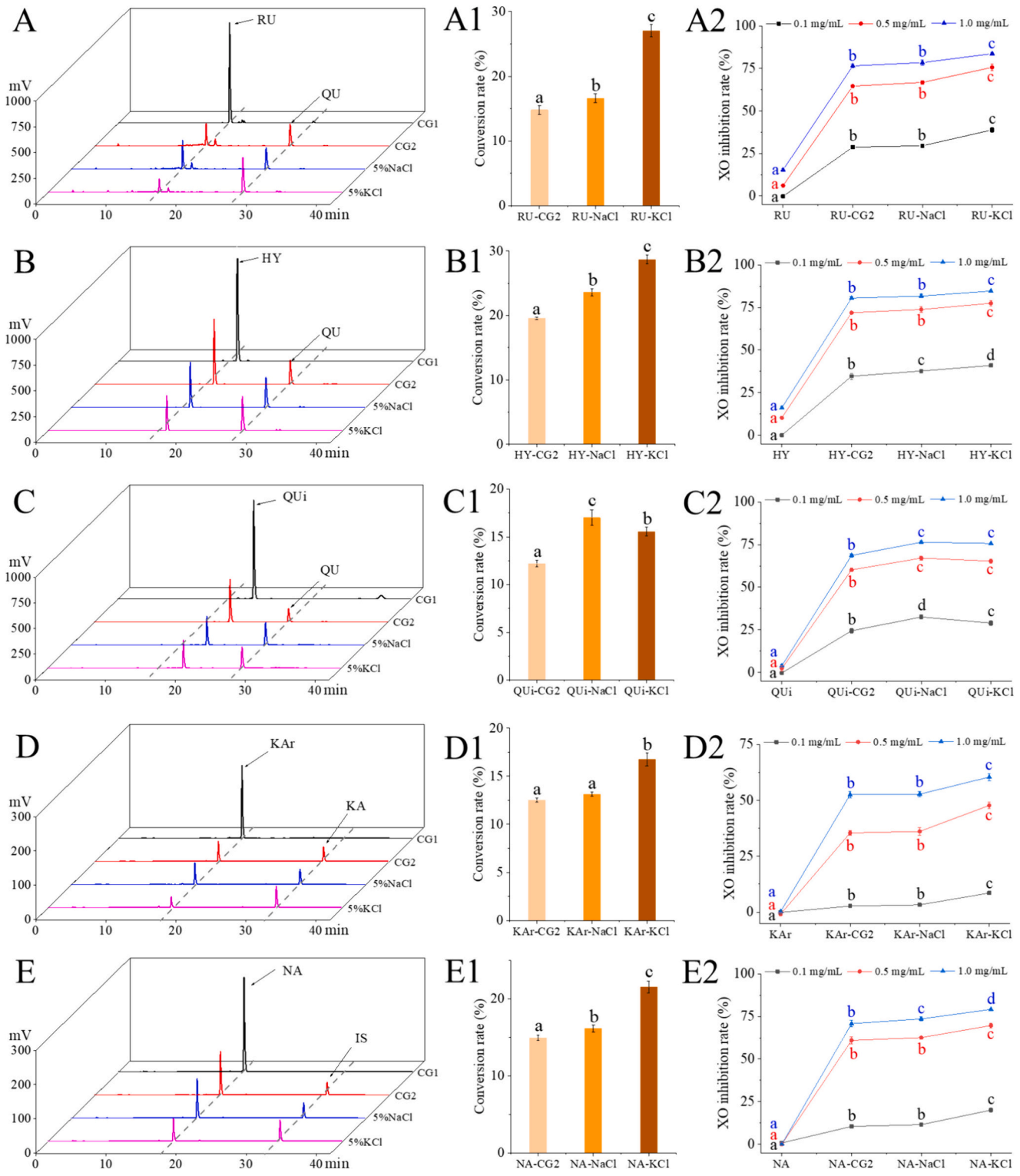

Fig. 3. Liquid chromatograms, conversion rate, and XO inhibition rate of rutin (A, A1, A2), hyperoside (B, B1, B2), quercitrin (C, C1, C2), kaempferol–3–O–rutinoside (D, D1, D2), narcissoside (E, E1, E2) before and after salt-assisted heat treatment. Different letters in the same graph or curve indicate significant differences ($p < 0.05$).

maximum degradation rate at these conditions. Meanwhile, the generation rate of QU reached the maximum at 180 °C with the k value of −0.0050. Similarly, the maximum degradation rate of KAr and NA reached the maximum at 200 °C, while the maximum generation rate of KA (k = −0.0042) and IS (k = −0.0038) was 160 °C. Interestingly, under the same conditions, the degradation rates of RU, KAr, and NA during KCl-assisted heat treatment were higher than those of ultrasound-assisted heat treatment, as well as the generation rates of QU, KA, and IS exhibited a similar trend (Li et al., 2023a). This phenomenon further indicated that KCl might enhance the conversion rate by accelerating the degradation and conversion of flavonoids during the heat treatment. In addition, the activation energy was calculated to evaluate the

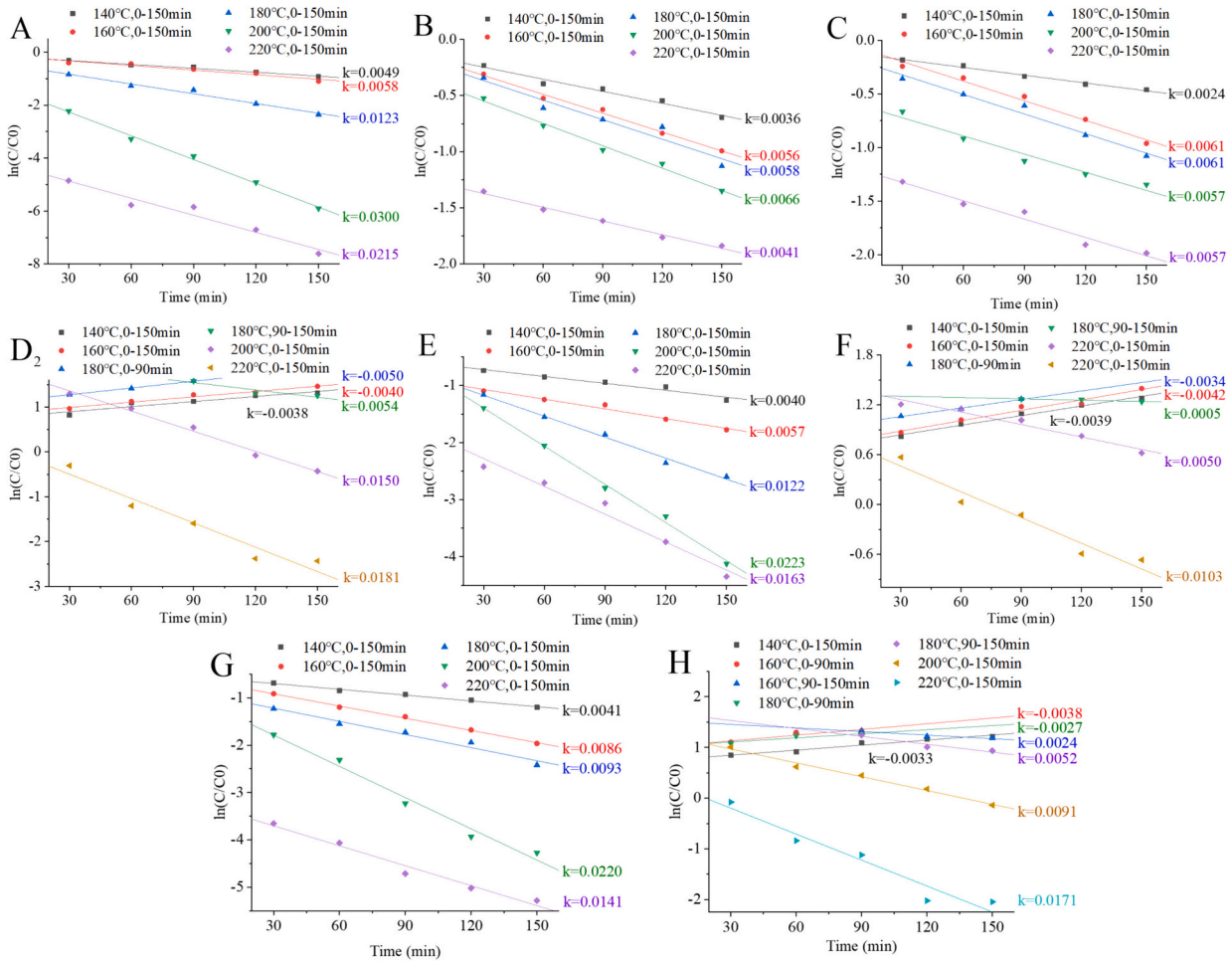

Fig. 4. First-order kinetics plots of rutin (A), hyperoside (B), quercitrin (C), quercetin (D), kaempferol–3–O–rutinoside (E), kaempferol (F), narcissoside (G), and isorhamnetin (H) contents in *Flos Sophorae Immaturus* tea extract treated at different temperatures.

degradation rates of different flavonoids, and the smaller the activation energy indicated the lower the initiation reaction energy and the faster the reaction rate (Abi-Khattar et al., 2022). As shown in Table 1, HY and QUi exhibited faster reaction rates, followed by NA, KAr, and RU, implying that the degradation rates of 3–*O*–rutinoside, 3–*O*–galactoside, and 3–*O*–rhamnoside were different. Previous studies found that the degradation rate of cyanidin–3–glucoside at 110 °C was the fastest, followed by cyanidin–3–rutinoside, cyanidin–3–sophoroside, cyanidin–3–glucorutinoside (Verbeyst, Crombruggen, Van der Plancken, Hendrickx, & Van Loey, 2011). Similar studies also showed that the degradation rates of three flavonoids under 130 °C heat treatment were as follows: Quercetin–3–*O*–rutinoside (k = 0.1590) > Luteolin–7–*O*–glucoside (k = 0.0744) > Naringenine–7–*O*–rhamnosidoglucoside (k = 0.0019). The presence of a double bond in the C-ring might be the reason that quercetin–3–*O*–rutinoside was more sensitive to temperature than naringenine–7–*O*–rhamnosidoglucoside, and additional energy was needed to break it (Chaaban et al., 2017). Meanwhile, the different molecule structure and glycosylation sites also induced different binding energy (Ali et al., 2019). Additionally, a degradation trend was observed when QU and KA were treated at 180 °C for more than 90 min, while IS also showed degradation trend at 160 °C for more than 90 min. All flavonoids showed significant degradation trend at 200 °C, indicating that appropriate heat treatment time and temperature were crucial factors in improving the generation rate of QU, KA, and IS.

3.6. ANN model construction

The effect of heat treatment on the flavonoids of FSIt mainly depended on time and temperature. However, suitable heat treatment conditions could not be determined through a few experiments, including various combinations such as low-temperature with long-term treatment or high-temperature with short-term treatment. Therefore, this study introduced ANN to predict the changes in FSIt flavonoids during KCl-assisted heat treatment. ANN is a nonlinear mathematical model constructed by simulating the processing mechanism of the human brain nervous system for complex information (Yu, Zheng, & Lin, 2022). Based on network topology knowledge, it possessed unique knowledge representation and adaptive learning ability, and exhibited good optimization and prediction ability in practical applications (Ciric, Krajnc, Heath, & Ogrinc, 2020). Therefore, a network was generated and comprised of one input layer (temperature, time), four hidden layers, and one output layer (RU, HY, QUi, QU, KAr, KA, NA, IS) (Fig. 5A). The number of hidden layers and prediction accuracy of the network were significantly correlated with training time, fault tolerance, and generalization ability. Too few hidden layers induced a decrease in generalization ability and prediction accuracy. On the contrary, excessive hidden layers induced convergence falling into local minima. Moreover, the number of neurons in each layer also significantly affected the prediction accuracy (Patruni & Rao, 2023). Therefore, the optimal model was established through multiple iterations with 4 hidden layers, and 128, 256, 256, and 128 hidden neurons per layer, respectively.

The ANN model tended to stabilize with the number of iterations

Table 1
Kinetics parameters of flavonoids degradation or generation during heating treatment.

Compound	Conditions	R^2	$t_{1/2}$ (min)	Ea (kJ/mol)
Rutin	140 °C, 0–150 min	0.9855	140.31	39.03
	160 °C, 0–150 min	0.9417	119.10	
	180 °C, 0–150 min	0.9792	56.40	
	200 °C, 0–150 min	0.9957	23.10	
	220 °C, 0–150 min	0.9536	32.22	
Hyperoside	140 °C, 0–150 min	0.9742	193.62	16.38
	160 °C, 0–150 min	0.9910	123.56	
	180 °C, 0–150 min	0.9321	119.51	
	200 °C, 0–150 min	0.9899	104.39	
	220 °C, 0–150 min	0.9874	170.31	
Quercitrin	140 °C, 0–150 min	0.9896	285.25	14.54
	160 °C, 0–150 min	0.9833	113.82	
	180 °C, 0–150 min	0.9759	113.82	
	200 °C, 0–150 min	0.9620	122.68	
	220 °C, 0–150 min	0.9647	121.39	
Quercetin	140 °C, 0–150 min	0.8915	−183.37	
	160 °C, 0–150 min	0.9733	−175.04	
	180 °C, 0–90 min	0.9979	−138.63	
	180 °C, 90–150 min	0.8864	127.42	
	200 °C, 0–150 min	0.9891	46.18	
	220 °C, 0–150 min	0.9417	38.27	
Kaempferol–3–O–rutinoside	140 °C, 0–150 min	0.9538	172.00	35.76
	160 °C, 0–150 min	0.9776	122.03	
	180 °C, 0–150 min	0.9829	54.15	
	200 °C, 0–150 min	0.9958	31.10	
	220 °C, 0–150 min	0.9694	42.52	
Kaempferol	140 °C, 0–150 min	0.9864	−180.04	
	160 °C, 0–150 min	0.9693	−166.22	
	180 °C, 0–90 min	0.9649	−203.27	
	180 °C, 90–150 min	0.8952	1318.82	
	200 °C, 0–150 min	0.9591	138.63	
	220 °C, 0–150 min	0.9451	67.23	
Narcissoside	140 °C, 0–150 min	0.9928	170.31	29.48
	160 °C, 0–150 min	0.9969	80.60	
	180 °C, 0–150 min	0.9620	76.00	
	200 °C, 0–150 min	0.9811	31.51	
	220 °C, 0–150 min	0.9738	49.30	
Isorhamnetin	140 °C, 0–150 min	0.9591	−209.41	
	160 °C, 0–90 min	0.8506	−184.84	
	160 °C, 90–150 min	0.9096	294.96	
	180 °C, 0–90 min	0.8132	−258.64	
	180 °C, 90–150 min	0.9161	133.30	
	200 °C, 0–150 min	0.9876	76.09	
	220 °C, 0–150 min	0.9408	40.61	

increasing. The lowest RMSE for training, validation, and testing groups were 1.86, 1.82, and 1.30, respectively (Fig. 5B). The error of the model presented a normal distribution with the average value of 0, and the error of most values was within ±0.5 (Fig. 5C). The R^2 between actual and predicted flavonoids content by ANN model were 0.9989 for RU, 0.9989 for HY, 0.9971 for QUi, 0.9943 for QU, 0.9915 for KAr, 0.9945 for KA, 0.9739 for NA, 0.9214 for IS (Fig. 5D). The model established through ANN presented a lower RSME, and the predicted results possessed a good correlation with the actual values, indicating that the ANN model possessed good predictive stability and ability (Kashyap, Riar, & Jindal, 2020). Thus, ANN was a promising approach to analyze and predict the changes in flavonoids content of FSIt during salt-assisted heat treatment.

4. Conclusion

Overall, salt-assisted heat treatment was confirmed to be an effective processing method for enhancing the XO inhibitory activity of FSIt. KCl could serve as catalysts to effectively promote the de-glycosylation of flavonoids during heat treatment. There were three main pathways for the de-glycosylation of flavonoids in FSIt: (1) the 3–*O*–rutinoside of RU, KAr, and NA degraded and converted to QU, KA, and IS; (2) the 3–*O*–galactoside of HY degraded and converted to QU; (3) the 3–*O*–rhamnoside of QUi degraded and converted to QU. The newly generated QU, KA, and IS exhibited better XO inhibitory activity than their glycosylation compounds, which might be the primary mechanism by which salt-assisted heat treatment enhances the XO inhibitory activity of FSIt. In addition, KCl was a more effective de-glycosylation catalyst than NaCl. KCl can replace NaCl in food industry, which is beneficial for humans who limit sodium intake. Moreover, KCl also possesses the industrial benefits of improving food texture, regulating acid-base balance, and preserving freshness. The degradation of flavonoids in FSIt during KCl-assisted heat treatment followed a first-order kinetic model, and appropriate heating time and temperature were the critical factors for promoting the conversion of flavonoids. A promising strategy for predicting the flavonoids content of FSIt was further established through the ANN model. This study provides a theoretical basis and technical support for the processing of FSIt products with good XO inhibitory activity.

CRediT authorship contribution statement

Jun Li: Writing – original draft, Methodology, Data curation, Conceptualization. **Peng Wu:** Software. **Jing Wang:** Software. **Xiangren Meng:** Writing – review & editing, Methodology. **Yang Ni:** Software, Funding acquisition. **Liuping Fan:** Writing – review & editing, Supervision, Funding acquisition, Conceptualization.

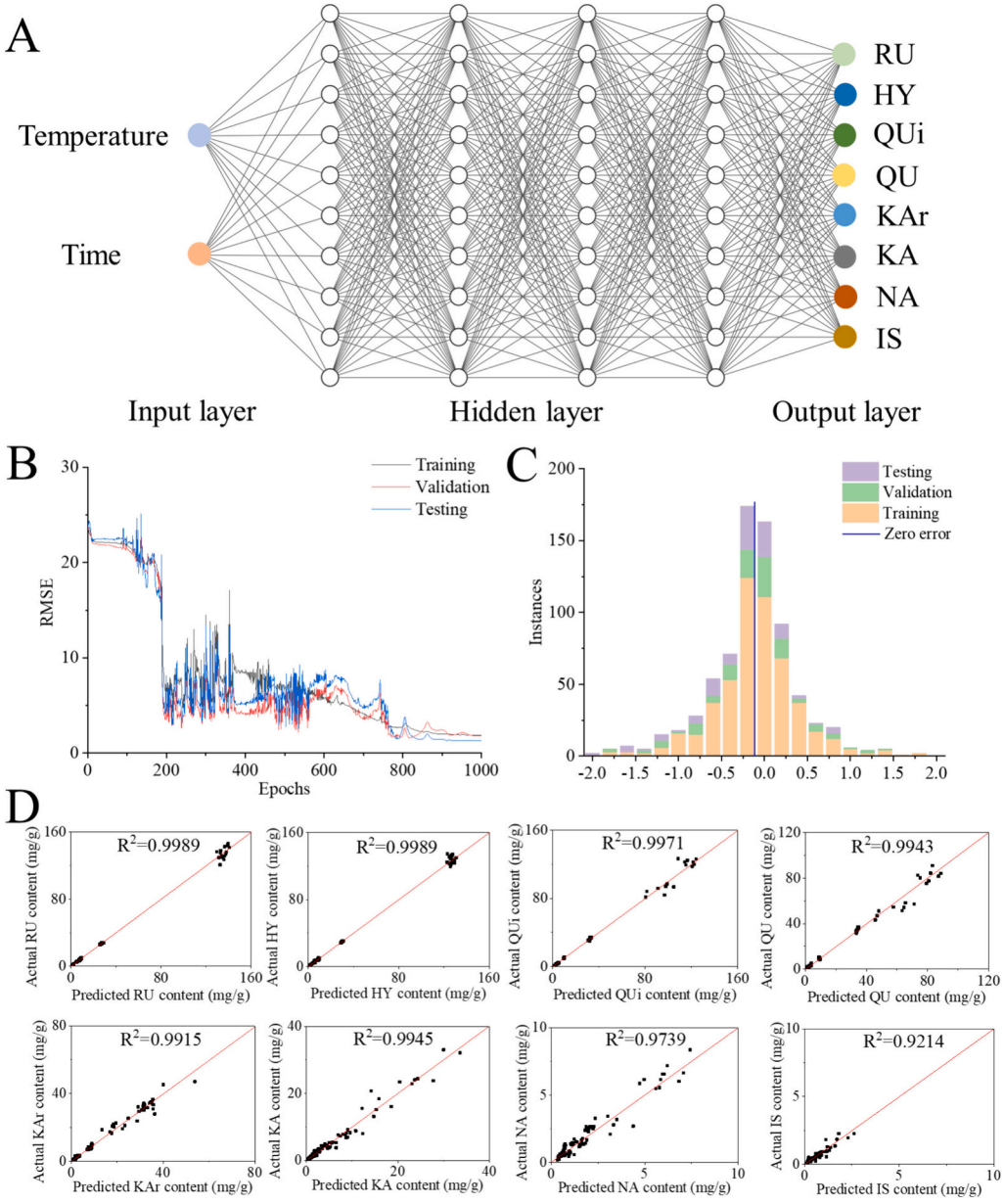

Fig. 5. (A) Training numbers of artificial neural networks model; (B)-(C) Establishment and performance of artificial neural networks model based on KCl-assisted treatment temperature and time; (D) Correlation coefficient of model prediction ability, predicted contents from treatments (after the treatments) vs. actual contents from control (without treatments).

Declaration of competing interest

The authors declare that they have no known competing financial interests or personal relationships that could have appeared to influence the work reported in this paper.

Data availability

Data will be made available on request.

Acknowledgments

The authors acknowledge financial support of the key research and development program of Xinjiang Autonomous Region (2022B02026-5), the China National Natural Science Foundation (32302117), Science and Technology Program of Guizhou Province (Qian Ke He Cheng Guo [2024] 052), which have enabled us to accomplish this study.

Appendix A. Supplementary data

Supplementary data to this article can be found online at https://doi.org/10.1016/j.fochx.2024.101854.

References

Abbas, A., & Alkheraije, K. A. (2023). Immunomodulatory effects of *carica papaya* extract against experimentally induced coccidiosis in broiler chickens. *Pakistan Veterinary Journal, 43*(3), 628–632.

Abduallah, A. M., Ahmed, A. E., Bajaber, M. A., & Alalwiat, A. A. (2023). Evaluation of the antidiabetic effects of methanolic extracts of neem (*Azadirachta indica*) seeds on the streptozotocin-induced wistar rats. *Pakistan Veterinary Journal, 43*(4), 792–798.

Abi-Khattar, A. M., Boussetta, N., Rajha, H. N., Abdel-Massih, R. M., Louka, N., Maroun, R. G., … Debs, E. (2022). Mechanical damage and thermal effect induced by ultrasonic treatment in olive leaf tissue. Impact on polyphenols recovery. *Ultrasonics Sonochemistry, 82*, Article 105895.

Ali, M. Y., Jannat, S., Edraki, N., Das, S., Chang, W. K., Kim, H. C., … Chang, M. S. (2019). Flavanone glycosides inhibit beta-site amyloid precursor protein cleaving

enzyme 1 and cholinesterase and reduce Abeta aggregation in the amyloidogenic pathway. *Chemico-Biological Interactions, 309*, Article 108707.
Bai, X., Zhang, M., Zhang, Y., Zhang, J., Wang, C., & Zhang, Y. (2021). Effect of steam, microwave, and hot-air drying on antioxidant capacity and *in vitro* digestion properties of polyphenols in oat bran. *Journal of Food Processing and Preservation, 45*(12), Article e16013.
Bebas, W., Gorda, I. W., & Agustina, K. K. (2023). Spermatozoa quality of Kintamani dogs in coconut water-egg yolk diluent with addition of Moringa leaves and carrot extract. *International Journal of Veterinary Science, 12*(3), 333–340.
Chaaban, H., Ioannou, I., Chebil, L., Slimane, M., Gérardin, C., Paris, C., … Ghoul, M. (2017). Effect of heat processing on thermal stability and antioxidant activity of six flavonoids. *Journal of Food Processing and Preservation, 41*(5), Article e13203.
Chao, E., & Fan, L. (2023). Changes in polyphenolic compounds and antioxidant activities of seed-used pumpkin during hydrothermal treatment. *Food Chemistry, 414*, Article 135646.
Chen, L. L., Verpoorte, R., Yen, H. R., Peng, W. H., Cheng, Y. C., Chao, J., & Pao, L. H. (2018). Effects of processing adjuvants on traditional Chinese herbs. *Journal of Food and Drug Analysis, 26*(2S), S96–S114.
Ciric, A., Krajnc, B., Heath, D., & Ogrinc, N. (2020). Response surface methodology and artificial neural network approach for the optimization of ultrasound-assisted extraction of polyphenols from garlic. *Food and Chemical Toxicology, 135*, Article 110976.
Dalal, D., Kunte, S., Oblureddy, V. T., & Anjali, A. K. (2023). Comparative evaluation of antimicrobial efficacy of german chamomile extract, tea tree oil, and chlorhexidine as root canal irrigants against e-faecalis and *streptococcus mutans* - an *in vitro* study. *International Journal of Agriculture and Biosciences, 12*(4), 252–256.
Dhlakama, N., Chawafambira, A., & Tsotsoro, K. (2022). Polyphenols, antioxidant activity, and functional properties of baobab (*Adansonia digitata* L) seeds soaked in monovalent ion salts. *International Journal of Food Properties, 25*(1), 1365–1376.
Doniec, J., Florkiewicz, A., Socha, R., & Filipiak-Florkiewicz, A. (2021). Polyphenolic acid content in Brassica vegetables during hydrothermal treatment with salt addition. *Journal of Food Processing and Preservation, 46*(2), Article e16219.
Gong, Y., Fan, L., Wang, L., & Li, J. (2023). *Flos Sophorae Immaturus*: Phytochemistry, bioactivities, and its potential applications. *Food Reviews International, 39*(6), 3185–3203.
He, X., Bai, Y., Zhao, Z., Wang, X., Fang, J., Huang, L., … Zheng, X. (2016). Local and traditional uses, phytochemistry, and pharmacology of *Sophora japonica* L.: A review. *Journal of Ethnopharmacology, 187*, 160–182.
Huo, D., Xiao, X., Zhang, X., Hao, X., Hao, Z., & Li, E. (2023). Exploration of unique starch physicochemical properties of novel buckwheat lines created by crossing Golden buckwheat and Tatary buckwheat. *Food Chemistry: X, 20*, Article 100949.
Jia, M. Z., Fu, X. Q., Deng, L., Li, Z. L., & Dang, Y. Y. (2021). Phenolic extraction from grape (*Vitis vinifera*) seed via enzyme and microwave co-assisted salting-out extraction. *Food Bioscience, 40*, Article 100919.
Kashyap, P., Riar, C. S., & Jindal, N. (2020). Optimization of ultrasound assisted extraction of polyphenols from Meghalayan cherry fruit (*Prunus nepalensis*) using response surface methodology (RSM) and artificial neural network (ANN) approach. *Journal of Food Measurement and Characterization, 15*(1), 119–133.
Kim, A. N., Kim, O. W., & Kim, H. (2022). Degradation kinetics of physicochemical and sensory properties of rice during storage at different temperatures. *Lwt, 164*, Article 113688.
Kim, D. S., & Lim, S. B. (2017). Optimization of subcritical water hydrolysis of rutin into isoquercetin and quercetin. *Preventive Nutrition and Food Science, 22*(2), 131–137.
Li, J., Gong, Y., Li, J., & Fan, L. (2023). Hydrothermal treatment improves xanthine oxidase inhibitory activity and affects the polyphenol profile of *Flos Sophorae Immaturus*. *Journal of the Science of Food and Agriculture, 1032*, 1205–1215.
Li, J., Gong, Y., Li, J., & Fan, L. (2023a). Improving the xanthine oxidase and adenosine deaminase inhibitory activities of *Flos Sophorae Immaturus* by ultrasound-assisted heating treatments. *Food Bioscience, 51*, Article 102245.
Li, J., Gong, Y., Li, J., & Fan, L. (2023b). Stir-frying treatment improves the color, flavor, and polyphenol composition of *Flos Sophorae Immaturus* tea. *Journal of Food Composition and Analysis, 116*, Article 105045.
Li, R. L., Zhang, Q., Liu, J., He, L. Y., Huang, Q. W., Peng, W., & Wu, C. J. (2021). Processing methods and mechanisms for alkaloid-rich Chinese herbal medicines: A review. *Journal of Integrative Medicine, 19*(2), 89–103.
Lin, S., Zhang, G., Liao, Y., Pan, J., & Gong, D. (2015). Dietary flavonoids as xanthine oxidase inhibitors: Structure-affinity and structure-activity relationships. *Journal of Agricultural and Food Chemistry, 63*(35), 7784–7794.
Liu, N., Wang, Y., Zeng, L., Yin, S., Hu, Y., Li, S., … Yang, X. (2020). RDP3, a novel antigout peptide derived from water extract of rice. *Journal of Agricultural and Food Chemistry, 68*(27), 7143–7151.
Mubaiwa, J., Fogliano, V., Chidewe, C., & Linnemann, A. R. (2019). Influence of alkaline salt cooking on solubilisation of phenolic compounds of bambara groundnut (*Vigna subterranea* (L.) Verdc.) in relation to cooking time reduction. *Lwt, 107*, 49–55.
Patruni, K., & Rao, P. S. (2023). Viscoelastic behaviour, sensitivity analysis and process optimization of *aloe Vera*/HM pectin mix gels: An investigation using RSM and ANN and its application to food gel formulation. *Lwt, 176*, Article 114564.
Premathilaka, R., Rashidinejad, A., Golding, M., & Singh, J. (2022). Oral delivery of hydrophobic flavonoids and their incorporation into functional foods: Opportunities and challenges. *Food Hydrocolloids, 128*, Article 107567.
Saleh, M., Ramadan, M., Elmadawy, R., Morsi, M., & El-Akabawy, L. (2023). The efficacy of alcoholic extracts of Morus macroura (mulberries), *Lepidium sativum* (garden cress seeds) and diclazuril against E. stiedae in experimentally infected rabbits. *International Journal of Veterinary Science, 12*(6), 869–878.
Sasaki, M., Manalu, H. T., Kamogawa, R., Issasi, C. S. C., Quitain, A. T., & Kida, T. (2023). Fast and selective production of quercetin and saccharides from rutin using microwave-assisted hydrothermal treatment in the presence of graphene oxide. *Food Chemistry, 405*(Pt B), Article 134808.
Singh, J. V., Mal, G., Kaur, G., Gupta, M. K., Singh, A., Nepali, K., … Pm, S. B. (2019). Benzoflavone derivatives as potent antihyperuricemic agents. *Medchemcomm, 10*(1), 128–147.
Sui, X., Yap, P. Y., & Zhou, W. (2015). Anthocyanins during baking: Their degradation kinetics and impacts on color and antioxidant capacity of bread. *Food and Bioprocess Technology, 8*(5), 983–994.
Turan, I., Canbolat, D., Demir, S., Kerimoglu, G., Colak, F., Alemdar, N. T., … Aliyazicioglu, Y. (2023). An investigation of the protective effect of *rhododendron luteum* extract on cisplatin-induced DNA damage and nephrotoxicity and biochemical parameters in rats. *Pakistan Veterinary Journal, 43*(3), 442–448.
Ulger, Y., & Delik, A. (2023). Artificial intelligence model with deep learning in nonalcoholic fatty liver disease diagnosis: Genetic based artificial neural networks. *Nucleosides, Nucleotides & Nucleic Acids, 42*(5), 398–406.
Verbeyst, L., Crombruggen, K. V., Van der Plancken, I., Hendrickx, M., & Van Loey, A. (2011). Anthocyanin degradation kinetics during thermal and high pressure treatments of raspberries. *Journal of Food Engineering, 105*(3), 513–521.
Wang, G., Cui, Q., Yin, L. J., Li, Y., Gao, M. Z., Meng, Y., … Wang, W. (2020). Negative pressure cavitation based ultrasound-assisted extraction of main flavonoids from *Flos Sophorae Immaturus* and evaluation of its extraction kinetics. *Separation and Purification Technology, 244*, Article 115805.
Xiao, K., & Tang, Y. (2021). Effect of dispersion and ion concentration on radio frequency heating. *Innovative Food Science & Emerging Technologies, 67*, Article 102552.
Xie, Y., Gong, T., Liu, H., Fan, Z., Chen, Z. J., & Liu, X. (2022). *In vitro* and *in vivo* digestive fate and antioxidant activities of polyphenols from hulless barley: Impact of various thermal processing methods and beta-glucan. *Journal of Agricultural and Food Chemistry, 70*(25), 7683–7694.
Xie, Z., Luo, X., Zou, Z., Zhang, X., Huang, F., Li, R., … Liu, Y. (2017). Synthesis and evaluation of hydroxychalcones as multifunctional non-purine xanthine oxidase inhibitors for the treatment of hyperuricemia. *Bioorganic & Medicinal Chemistry Letters, 27*(15), 3602–3606.
Yang, J., Shen, M., Wu, T., Luo, Y., Li, M., Wen, H., & Xie, J. (2020). Role of salt ions and molecular weights on the formation of Mesona chinensis polysaccharide-chitosan polyelectrolyte complex hydrogel. *Food Chemistry, 333*, Article 127493.
Yu, H., Zheng, J., & Lin, Q. (2022). Strength prediction of seawater sea sand concrete based on artificial neural network in python. *Materials Research Express, 9*(3), Article 035201.
Yu, Q., Fan, L., Duan, J., Yu, N., Li, N., Zhu, Q., & Wang, N. (2020). Ultrasound and heating treatments improve the antityrosinase ability of polyphenols. *Food Chemistry, 317*, Article 126415.
Zhang, Z., Li, J., Fan, L., & Duan, Z. (2020). Effect of organic acid on cyanidin-3-O-glucoside oxidation mediated by iron in model Chinese bayberry wine. *Food Chemistry, 310*, Article 125980.